

## Supplementary information

### Label-Free Differentiation of Living versus Dead Single Yeast Cells using Broadband Electrical Impedance Spectroscopy

Amirhossein Favakeh,<sup>1</sup> Amir Mokhtare,<sup>1</sup> Mohammad Javad Asadi,<sup>2</sup> James C. M. Hwang,<sup>2,3</sup>

Alireza Abbaspourrad\*<sup>1</sup>

<sup>1</sup>Food Science Department, College of Agriculture and Life Sciences (CALS), Cornell University, Ithaca 14853, New York, USA.

<sup>2</sup>School of Electrical and Computer Engineering, Cornell University, Ithaca, New York 14853, USA.

<sup>3</sup>Department of Materials Science and Engineering, Cornell University, Ithaca, New York 14853, USA.

\* Corresponding Author: Alireza Abbaspourrad, E-mail: [alireza@cornell.edu](mailto:alireza@cornell.edu)

#### Table of Contents

Supplementary information .....	1
Theory .....	2
Figure S1 Discussion .....	5
Figure S2 - ANSYS High-Frequency Structure Simulator (HFSS) Software Data .....	6
Fabrication of Microfluidic Channel .....	7
Figure S3 - Experiment setup .....	8
Discussion of Table S1 .....	9
Table S1. Electrical properties characterization of a yeast cell .....	10
Figure S4 - Reflection and transmission phase changes for live and dead single yeast .....	11
References .....	12

## Theory

Schwan introduced three primary dispersion mechanisms for the dielectric constant and tissue conductivity named  $\alpha$ ,  $\beta$ , and  $\gamma$  dispersions.<sup>1</sup> Later cell suspension dispersion mechanisms were added.<sup>2</sup> An  $\alpha$  dispersion occurs at low frequencies (below a few kHz) and is generally attributed to the diffusion processes of the ionic species present in biological fluids. A  $\beta$  dispersion happens at the megahertz frequency range and is attributed to the polarization occurring at the interfaces of cellular plasma membranes, additionally, the polarization is frequency-dependent and shows relaxations. A  $\gamma$  dispersion is attributed to the vibration of water-free molecules and small biological molecules within the gigahertz frequency range.<sup>3</sup>

In this study,  $\beta$  dispersion has been shown across the frequency range between 30 kHz to 6 GHz. For simplicity, we defined a single-shell spherical model for yeast. (**Figure 3b**). We can represent each nondispersive parameter as follows:<sup>4,5</sup>

$$R_{YM} = d_{YM}/\sigma_{YM} d_c^2 \approx 0.5 \text{ M}\Omega \quad (1)$$

$$C_{YM} = k_{YM}\epsilon_0 d_c^2/d_{YM} \approx 0.25 \text{ pF} \quad (2)$$

$$R_{CP} = 1/d_C \sigma_{CP} \approx 0.18 \text{ M}\Omega \quad (3)$$

$$C_{CP} = k_{CP}\epsilon_0 d_C \approx 2.5 \text{ fF} \quad (4)$$

Where  $k$  is the dielectric constant,  $\sigma$ , is the conductivity, and  $\epsilon_0 = 8.854 \times 10^{-12}$  F/m is the vacuum permittivity,  $d_c$  is the cell diameter, and  $d_{YM}$  is the membrane thickness. These properties for yeast membrane and cytoplasm are considered as  $d_{YM} \approx 7 \text{ nm}$ ,<sup>6</sup>  $d_C \approx 5.5 \text{ }\mu\text{m}$ ,<sup>7</sup>  $k_{YM} \approx 6.8$ ,<sup>8</sup>  $k_{CP} \approx 50$ ,<sup>9</sup>  $\sigma_{YM} \approx 4.5 \times 10^{-4} \text{ S/m}$ ,<sup>6</sup> and  $\sigma_{CP} \approx 1 \text{ S/m}$ .<sup>7</sup>

The system's complex impedance ( $Z$ ) is determined as a function of the voltage to the

current ratio ( $Z(j\omega) = \frac{V(j\omega)}{I(j\omega)}$ ), where  $j = \sqrt{-1}$ ,  $V$  is voltage,  $I$  is the current, and  $\omega$  is angular frequency. This complex impedance can be expressed as follows:

$$Z = Z_{Re} + jZ_{Im} \quad (5)$$

where

$$Z_{Re} = R \quad (6)$$

$$Z_{Im} = -\frac{1}{\omega C} \quad (7)$$

where  $R$  is resistance,  $C$  is capacitance and  $\omega$  angular frequency. The imaginary impedance ( $Z_{Im}$ ) and real impedance ( $Z_{Re}$ ) represent a circuit's capability to store electrical energy (imaginary) and resist current flow (real), respectively. A cell can be represented as a complex impedance; therefore, based on **Figure 3b**, the impedance of a parallel resistance and capacitance can be expressed as

$$\frac{1}{Z} = j\omega C + \frac{1}{R} = \frac{1 + j\omega CR}{R} \quad (8)$$

then

$$Z = \frac{R}{1 + j\omega CR} = \frac{R}{1 + j\omega CR} \times \frac{1 - j\omega CR}{1 - j\omega CR} = \frac{R - j\omega CR^2}{1 + (\omega CR)^2} \quad \text{and} \quad \omega_0 = \frac{1}{RC} \quad (9)$$

then

$$Z = \frac{R - jR(\omega/\omega_0)}{1 + (\omega/\omega_0)^2} = \frac{R}{1 + (\omega/\omega_0)^2} - j \frac{R(\omega/\omega_0)}{1 + (\omega/\omega_0)^2} \quad (10)$$

therefore, the yeast impedance is:

$$Z = \frac{2R_{YM}}{1 + (\omega/\omega_{YM})^2} + \frac{R_{CP}}{1 + (\omega/\omega_{CP})^2} - j\frac{2R_{YM}(\omega/\omega_{YM})}{1 + (\omega/\omega_{YM})^2} - j\frac{2R_{CP}(\omega/\omega_{CP})}{1 + (\omega/\omega_{CP})^2} \quad (11)$$

where  $\omega$  is an angular frequency when  $f$  is the applied electromagnetic frequency signal is

$$\omega = 2\pi f, \omega_{YM} = 1/R_{YM}C_{YM}, \text{ and } \omega_{CP} = 1/R_{CP}C_{CP}. \quad (12)$$

The admittance of a cell can be expressed as:

$$Y = 1/Z = G + j\omega C \quad (13)$$

where  $G = 1/R$  and  $C$  are the conductance and capacitance of the cell, which are proportional to the cell conductivity and cell dielectric constant, respectively. The admittance of a cell for a single shell model can be defined as:<sup>10</sup>

$$Y = \frac{(G_{YM} + j\omega C_{YM})(G_{CP} + j\omega C_{CP})/2}{(G_{YM} + j\omega C_{YM})/2 + (G_{CP} + j\omega C_{CP})} \approx \frac{[2G_{YM} + (\omega/\omega_0)^2 G_{CP}] + j\omega[2C_{YM} + (\omega/\omega_0)^2 C_{CP}]}{4 + (\omega/\omega_0)^2} \quad (14)$$

where  $G_{YM} = 1/R_{YM}$ ,  $G_{CP} = 1/R_{CP}$ , and  $\omega_0 = 1/R_{CP}C_{YM} \approx 20$  MHz ( $f_0 \approx 1$  MHz). Regarding dielectric spectroscopy, the complex permittivity of a cell as a homogenous dielectric particle can be defined as  $\varepsilon = k\varepsilon_0 - j\sigma/\omega$ , therefore:

$$Y = (\sigma + j\omega k\varepsilon_0) d_C \quad (15)$$

Equating the admittance formula:

$$\sigma \approx \frac{2G_{YM} + (\omega/\omega_0)^2 G_{CP}}{d_C[4 + (\omega/\omega_0)^2]} \quad (16)$$

$$k \approx \frac{2C_{YM} + (\omega/\omega_0)^2 C_{CP}}{\epsilon_0 d_C [4 + (\omega/\omega_0)^2]} \quad (17)$$

therefore,  $k$  and  $\sigma$  can be calculated by estimating  $R_{YM}$ ,  $C_{YM}$ ,  $R_{CP}$ ,  $C_{CP}$ , and  $d_C$ .

### Figure S1 Discussion

The  $\beta$  dispersion occurs around 1 MHz based on the parallel equivalent circuit of resistance and capacitance for yeast membrane and cytoplasm (**Figure S1**). The conductivity and dielectric constant values below and above the  $\beta$  dispersion correspond to  $R_{YM}$ ,  $C_{YM}$  and  $R_{CP}$ ,  $C_{CP}$ , respectively. At lower frequency ranges (kHz to MHz), the cell membrane acts as an insulator, and the electrical signals cannot penetrate the cell membrane. The measured impedance is only attributed to membrane resistance,  $R_{YM}$ , and capacitance  $C_{YM}$ , while at higher frequency ranges (above  $\sim 1$  MHz), signals penetrate through the membrane due to the slow response time of ions, and the impedance is attributed to the cytoplasm resistance  $R_{CP}$  and its associated capacitance  $C_{CP}$ .

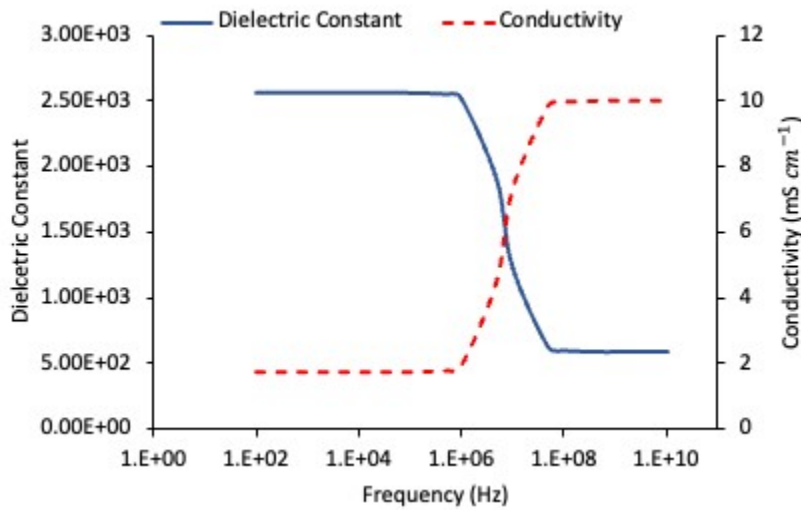


**Figure S1.** Dielectric constant and conductivity over the frequency spectrum for a single yeast. The hypothesis is based on parallel circuits of resistance and capacitance for the cell membrane and cytoplasm.

**Figure S2 - ANSYS High-Frequency Structure Simulator (HFSS) Software Data**

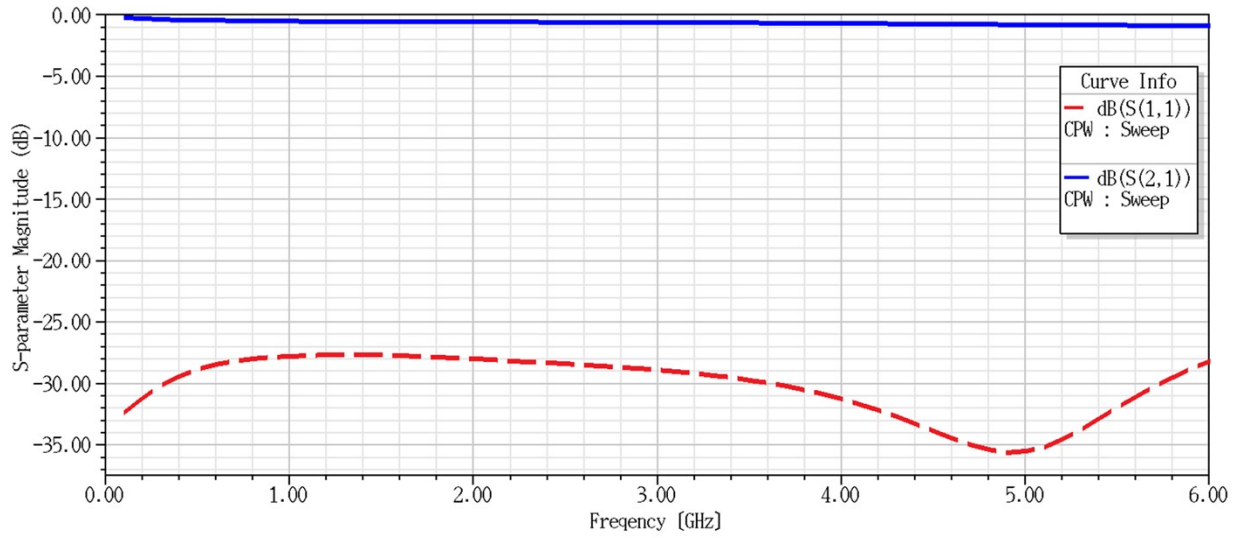
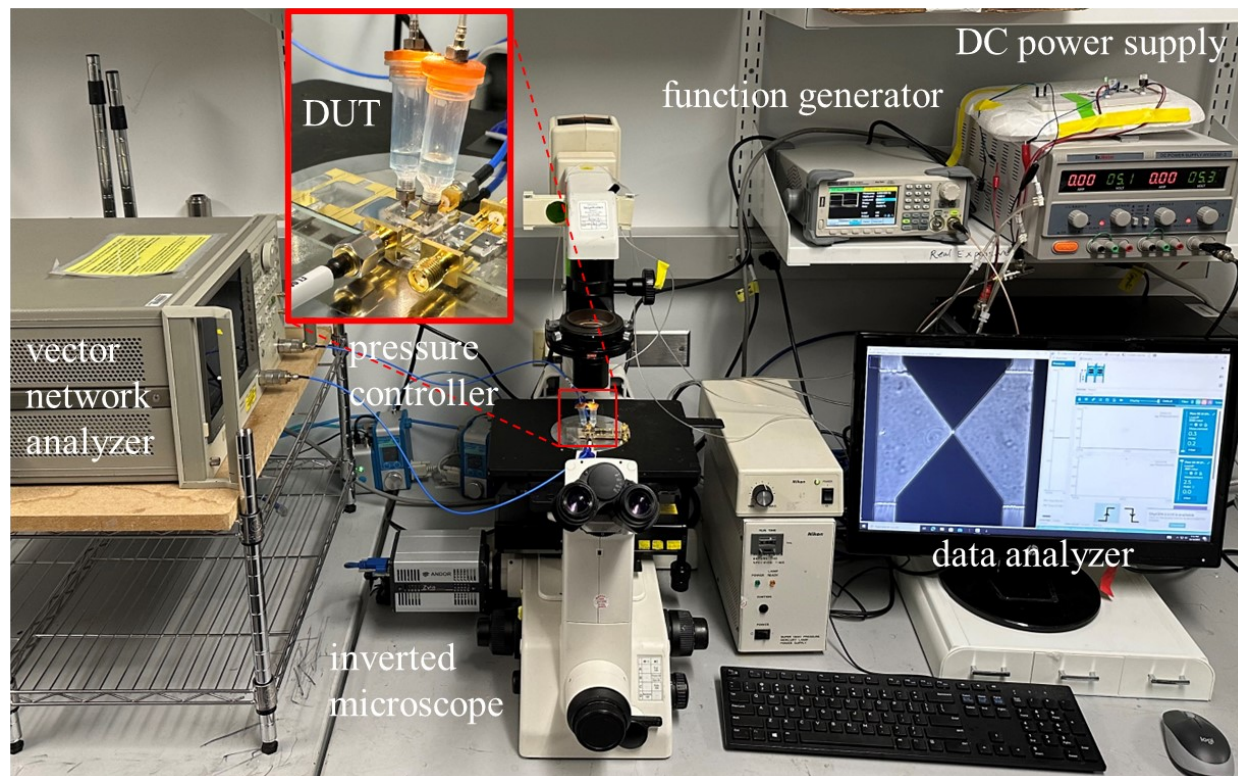


Figure S2. Reflection and transmission coefficients were simulated using ANSYS software's High-Frequency Structure Simulator (HFSS) for the CPW with three sets of transmission lines (thru). The amount of reflection loss is very low, and most of the signal has been transmitted.

### **Fabrication of Microfluidic Channel**

Microfluidic devices were fabricated using a one-step photolithography process<sup>11,12</sup>. First, the master mold for PDMS casting was fabricated with the SU8-2025 negative photoresist (Kyaku Advanced Materials INC Westborough, MA), followed by the recommended protocols spin-coated to the silicon wafer to achieve a 20-micron thick layer. After soft baking, exposure, and post-exposure baking, the developed pattern was hard-baked. Afterward, polydimethylsiloxane (PDMS, Dow Sylgard™ 184 Silicone Encapsulant Clear 0.5 KG Kit, Ellsworth Adhesive, Germantown, WI ) was poured on the patterned silicon wafer. Curing, peeling, and cutting the PDMS was the final step of the fabrication process. A microfluidic channel was molded onto the bottom side of the PDMS to cover the CPW sensing gap (**Figure 2c**).

**Figure S3 - Experiment setup**



**Figure S3.** Experiment setup. The device under test (DUT) is placed on the microscope stage and connected to the vector network analyzer (VNA).



## Discussion of Table S1

A comparison between the extracted data for the yeast equivalent circuit elements measured in this research with electrical properties values of different yeast cell lines in the literature was made. Most of the literature reports for cell suspensions were carried out in the frequency range of kHz to MHz. To facilitate the comparison, we converted the conductivity and dielectric constant values reported in the literature, which were measured by dielectric spectroscopy, to resistance and capacitance based on the single-cell simple cube shape, using **equation (1-4)**. We found that not only were our experimental results within the same order of magnitude as the literature, but they were also in general agreement with the estimated theoretical values. Considering the characterization method, different cell lines, and different cell sizes, this level of comparison is acceptable. Among all of the data we collected,  $R_{YM}$  shows the highest degree of deviance from the reported literature values for similar systems. The reason is due to the solution effect at lower frequencies, which we minimized by resuspending the cells in a low-conductive sucrose/dextrose solution.

Because most of the cytoplasm volume consists of water, we expected to measure the live yeast cytoplasm capacitance close to that of water. The water capacitance sandwiched between two parallel electrodes can be calculated as  $C = \frac{\epsilon_0 \epsilon_w A}{t}$  where  $\epsilon_0$  is the vacuum permittivity,  $\epsilon_0 = 8.854 \times 10^{-12}$  F/m,  $\epsilon_w$  is permittivity of water 80, the cross-sectional area is  $A = 5^2 \mu m^2$  and the distance between the electrodes is  $t = 5 \mu m$ . Our calculated water capacitance was 3.54 fF, which is close to our measure value.

**Table S1. Electrical properties characterization of a yeast cell**

Bandwidth (MHz)	$R_{YM}$ (M $\Omega$ )	$C_{YM}$ (pF)	$R_{CP}$ (M $\Omega$ )	$C_{CP}$ (fF)	Reference
0.001 - 100	56	0.3	0.6	3.3	13
0.1 - 1000	0.3	0.3	0.2	3.3	14
0.01 - 10	1	0.3	0.7	3.1	15
Nanosecond pulse	39	0.5	0.5	4	16
0.001 - 500	0.6	0.1	0.1	2.2	6
0.01 - 100	—	0.06	0.7	1.9	8
0.01 - 10000	—	0.2	0.3	2.4	9
Nanosecond pulse	50	0.4	0.4	3.5	17
0.001 - 1	88	0.2	0.8	2.6	18
0.03 - 6000	$0.17 \pm 0.08$	$0.3 \pm 0.1$	$0.10 \pm 0.04$	$3.6 \pm 0.1$	This work

**Figure S4 - Reflection and transmission phase changes for live and dead single yeast**

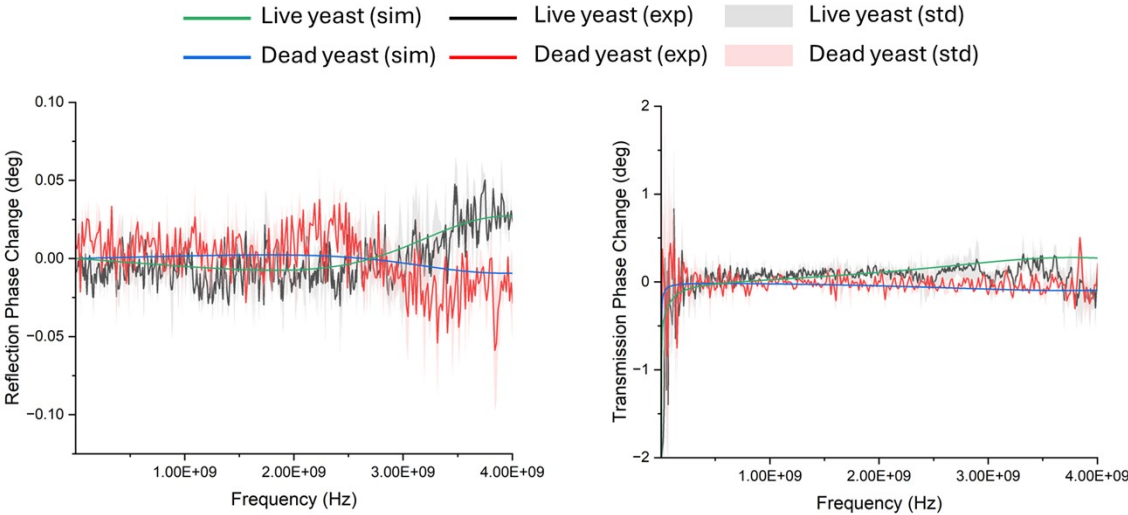


Figure S4 - (a) Reflection and (b) transmission phase changes for live and dead single yeast trapped between coplanar waveguide (CPW).

## References

- 1 H. P. Schwan, *IRE Trans. Med. Electron.*, 1955, **PGME-3**, 32–46.
- 2 H. P. Schwan, in *Advances in Biological and Medical Physics*, Elsevier, 1957, vol. 5, pp. 147–209.
- 3 H. P. Schwan, *IEEE Trans. Electr. Insul.*, 1985, **EI-20**, 913–922.
- 4 X. Ma, X. Du, H. Li, X. Cheng and J. C. M. Hwang, *IEEE Trans. Microw. Theory Tech.*, 2018, **66**, 3690–3696.
- 5 X. Du, X. Ma, H. Li, L. Li, X. Cheng and J. C. M. Hwang, *IEEE J. Electromagn. RF Microw. Med. Biol.*, 2019, **3**, 127–133.
- 6 N. Haandbæk, S. C. Bürgel, F. Heer and A. Hierlemann, *Lab Chip*, 2014, **14**, 369–377.
- 7 M. Kriegmaier, M. Zimmermann, K. Wolf, U. Zimmermann and V. L. Sukhorukov, *Biochim. Biophys. Acta BBA - Gen. Subj.*, 2001, **1568**, 135–146.
- 8 Koji, Asami, .
- 9 Asami Koji and S. Yonezawa, Takeshi, *Biophys. J.*, 1996, **71**, 2192–2200.
- 10 X. Ma, X. Du, L. Li, H. Li, X. Cheng and J. C. M. Hwang, *IEEE J. Electromagn. RF Microw. Med. Biol.*, 2020, **4**, 37–44.
- 11 M. A. Bijarchi, A. Favakeh, S. Alborzi and M. B. Shafii, *Sens. Actuators B Chem.*, 2021, **329**, 129274.
- 12 M. Yaghoobi, A. Abdelhady, A. Favakeh, P. Xie, S. Cheung, A. Mokhtare, Y. L. Lee, A. V. Nguyen, G. Palermo, Z. Rosenwaks, S. H. Cheong and A. Abbaspourrad, *Lab. Chip*, 2024, **24**, 210–223.
- 13 K. Zhao, Larasati, B. P. Duncker and D. Li, *Anal. Chem.*, 2019, **91**, 6304–6314.
- 14 R. Hölzel and I. Lamprecht, *Biochim. Biophys. Acta BBA - Biomembr.*, 1992, **1104**, 195–200.
- 15 Y. Huang, R. Holz, R. Pethig and X.-B. Wang, *Phys. Med. Biol.*, 1992, **37**, 1499–1517.
- 16 J. Fathy, A. Pourmand and H. B. Ghavifekr, *Microsyst. Technol.*, 2017, **23**, 1351–1360.
- 17 Z. Zhu, O. Frey, D. S. Ottoz, F. Rudolf and A. Hierlemann, *Lab Chip*, 2012, **12**, 906–915.
- 18 S. Patel, D. Showers, P. Vedantam, T.-R. Tzeng, S. Qian and X. Xuan, *Biomicrofluidics*, 2012, **6**, 034102.